

In Situ Gas Content Prediction Method for Shale

Ning Li,* Tongwen Jiang, and Wei Xiong

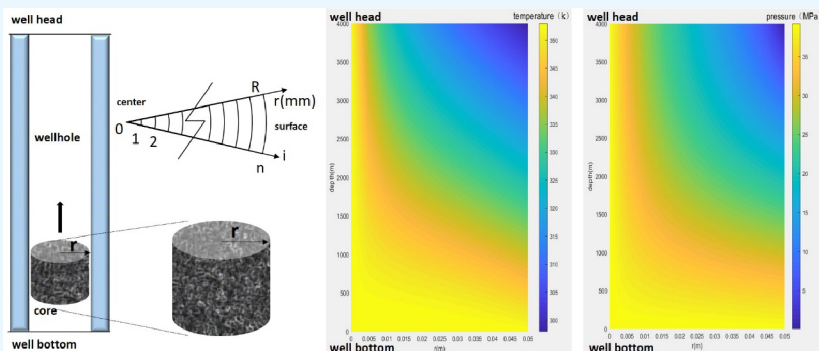
Cite This: *ACS Omega* 2024, 9, 16128–16137

Read Online

ACCESS |

Metrics & More

Article Recommendations



ABSTRACT: Shale gas is a typical unconventional energy source and recently has received great attention around the world. Unlike conventional natural gas, shale gas mainly exists in two forms: free state and adsorbed state. Therefore, geologists have proposed the concept of gas content. The traditional calculation methods of gas content can be summarized as on-site gas desorption, logging interpretation, isothermal adsorption, and so on. However, all of the methods mentioned above have their shortcomings. In situ gas content is a new concept in the calculation of the gas content. In this paper, the in situ gas content is defined as the gas content obtained by direct measurement of core gas production through experimental or mathematical simulation of original reservoir conditions. In this work, a method to calculate the in situ gas content of shale is provided, which includes two parts: numerical simulation of the coring process and a gas content experiment. Compared with previous gas content prediction methods, this article considers the influence of the temperature field on gas content both in mathematical modeling and experiments. Then, the gas content of the Longmaxi Formation shale in the Sichuan Basin was calculated using both methods as an example. The results show that (1) the numerical model was considered to be reliable by analyzing the effects of coring speed and permeability on the loss of gas; (2) the total gas content predicted by numerical simulation of the coring process and the gas content experiment are approximately equal, with values of 5.08 m³/t and 4.95 m³/t, respectively; (3) the total gas content of the USBM method is only 4.28 m³/t, which is significantly lower than the above methods. In summary, this study provides an in situ gas content prediction method for shale from both mathematical modeling and experiments. The mutual verification of theory and experiment makes this method highly reliable.

1. INTRODUCTION

With the increasing demand for energy over the years, there is an urgent need to develop unconventional oil and gas resources. Shale gas has become one of the leading natural gas resources in North America and China. The U.S. Energy Information Administration (EIA) estimates that in 2022, U.S. shale gas production was about 807 billion cubic meter (cbm). In the same year, China's shale gas production was about 24 billion cubic meter (cbm).

Gas content is a significant parameter for gas-bearing evaluation, sweet-spot selection, resource calculation, EUR prediction, economic evaluation, etc.^{1–3} As is known to all, the gas content can be analyzed by a number of methods qualitatively or quantitatively. These methods can be summarized as follows: (1) on-site gas desorption; (2) logging interpretation; (3) isothermal adsorption.⁴ Looking at various

types of gas content prediction methods, each has its own flaws.

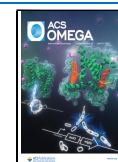
First, we used on-site gas desorption. After years of development, the measurements of desorbed gas are becoming more accurate. And the remaining gas content is getting smaller and smaller. However, too many errors and uncertainties occurred in the estimation of lost gas content, such as the USBM method⁵ and the ACF method⁶. So, the gas

Received: December 14, 2023

Revised: March 7, 2024

Accepted: March 12, 2024

Published: March 26, 2024



content obtained from on-site desorption is still questionable. Second, the logging interpretation. Predicting the gas content of shale or coal by means of logging interpretation^{7–10} is a serious challenge of conventional methods. These methods can calculate the gas content of shale quickly. But the disadvantages of these methods are also obvious. The logging interpretation method is an indirect method for calculating gas content, and its results are quite uncertain. Third, isothermal adsorption. The calculation of gas content in shale by the isothermal adsorption method began in the 1980s. But there are two problems in these methods: First, the specific surface of the shale powder is much larger than that of the core, resulting in a larger adsorption area. Second, methane adsorption reaches saturation under experimental conditions but may not reach saturation under real reservoir conditions. So, the results of isothermal adsorption represent only the maximum adsorption capacity. In conclusion, all of the methods mentioned above have their shortcomings.

According to previous research, the gas content of shale is affected by following many factors:^{11–17} 1) type, maturity, and abundance of organic matter; 2) mineral type and content of shale; 3) pore structure and pore volume; 4) formation temperature and pressure conditions. In situ conditions preserve the original state of the shale as much as possible. In this paper, in situ gas content is defined as the gas content obtained by direct measurement of core gas production through experimental or mathematical simulation of original reservoir conditions. That is to say, these methods emphasize the simulation of the original conditions, especially for temperature and pressure.

The significance of the in situ conditions for the calculation of gas content in this paper is reflected mainly in two aspects. First, the cooling shrinkage of the shale pore system is avoided.¹⁸ Therefore, the experimental porosity is similar to that of the original formation porosity. Therefore, the free gas content can be accurately simulated. Second, since the experimental temperature is equal to the formation temperature, the pore surface properties are the same as the formation conditions. So, the adsorbed gas content can be accurately simulated too. As it is well-known that shale gas is mainly composed of free gas and adsorbed gas. Therefore, this work can accurately predict the gas content of shale and then support the resource calculation and the formulation of gas field exploration solutions.

Previous studies have been conducted on the in situ gas content. There are two main types of in situ gas content prediction methods, namely, simulation of lost gas during coring^{1,17,19,20} and pressure-holding coring.²¹ The first type of method commonly tries to calculate the loss of gas during coring by building mathematical models. The total gas content of the shale can be obtained by adding the loss of gas and on-site desorption gas. However, the above methods have been widely questioned due to a lack of experimental verification. The second type of method attempts to maintain the core pressure during coring by using pressure-holding coring technology. If the core cylinder is well airtight, the gas released represents the gas content of the shale. But, the pressure-holding coring process is too expensive, so it is difficult to be widely used.

In this work, a new in situ gas content prediction method for shale is constructed and verified by calculating the gas content of the Longmaxi Formation shale in the Sichuan Basin, which includes two parts: numerical simulation and experiment. In

the example, the gas content of shale was calculated by numerical simulation and experiments, respectively. Then, the predicted results of the two parts together with the USBM method and pressure-holding coring are compared. The total gas content predicted by the numerical simulation of the coring process and the gas content experiment are approximately equal. The results of the USBM method and pressure-holding coring are lower than that. In order to further verified the practicability of the numerical model. The model is used to analyze the effects of the clogging speed and core permeability on the loss of gas, and the results are considered to be reliable. In other words, the combination of numerical simulation and experiment makes the gas content of shale predicted by the new method reliable and accurate.

2. METHODS

Based on the above analysis, this work aims to provide a method to calculate the in situ gas content of shale. This method includes two parts: the numerical simulation of the coring process and the gas content experiment. In the first part, the total gas content is calculated by simulating the loss of gas during coring. In the second part, we simulate the original formation conditions, measure the core gas production by experiments, and then calculate the total gas content. The numerical simulation method (part 1) and the experimental method (part 2) are mutually verified.

2.1. Gas Content Prediction Method Based on the Coring Process. During heating, the loss of methane varies with pressure and temperature. In order to calculate the loss of methane in the coring process, a mathematical model is established and the numerical calculation is made. The core is considered to be a cylinder in this model, as shown in Figure 1.

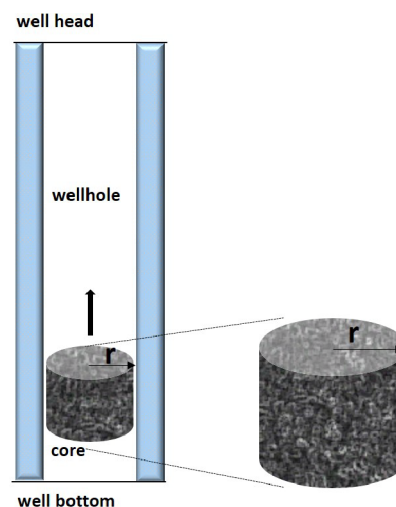


Figure 1. Diagram of the coring process.

The gas composition of shale gas is mainly methane, and the occurrence mode is the coexistence of free gas and adsorbed gas.^{22,23} The microscopic flow mechanism of shale gas is very complicated. But it is generally believed that under typical shale gas reservoir conditions, shale gas flows are mainly viscous flow, slippage flow, and weak transition flow.^{24,25} That is to say, the microscopic flow of shale roughly follows Darcy's law. Due to the short duration of the coring process, generally 3–5 h, the change of porosity during the coring process is ignored in this study. As for the seepage direction of methane

in the core, since the length of the core is much larger than the diameter, the pressure gradient is mainly reflected in the radial direction. There is a large amount of adsorbed gas in the core. The desorption of adsorbed gas can maintain the core pressure, and the duration of the coring process is short. So, this study assumes that the core center is the constant pressure boundary.

The model is based on the following basic assumptions:

1. Shale gas contains only methane and no other chemical components.
2. Methane exists in the core pores in the form of free gas and adsorbed gas.
3. Methane flow in the core pores is consistent with Darcy's law.
4. Core porosity remains constant during coring.
5. Methane escapes radially through the core, ignoring its axial flow.
6. The temperature and pressure of the core center remain constant during coring.

Based on the above assumptions, the flow of free gas in the core is simplified as a one-dimensional radial seepage. In this part, the calculation of the temperature field and pressure field will be discussed, respectively.

2.1.1. Temperature Field. The heat conduction equation in polar coordinates is shown as follow:²⁶

$$\frac{\partial T}{\partial t} = \frac{1}{r} \frac{\partial}{\partial r} \left(r \frac{\partial T}{\partial r} \right) = \frac{\partial^2 T}{\partial r^2} + \frac{1}{r} \frac{\partial T}{\partial r} \quad (1)$$

where T is temperature, t is time, and r is distance from the core center.

The initial condition is shown as follow:

$$T|_{t=0} = T_w (0 \leq r \leq R_c) \quad (2)$$

where T_w is well bottom temperature.

It is assumed that the core center temperature is always equal to the formation temperature, and the core surface temperature is equal to the mud temperature. The boundary conditions are shown as follows:

$$T|_{r=r_c} = T_c (t \geq 0) \quad (3)$$

$$T|_{r=0} = T_w (t \geq 0) \quad (4)$$

where r_c is the radius of core and T_c is the mud temperature.

The core surface temperature is always equal to the temperature of the drilling mud at the same depth. So, the subsidiary equation is shown as follow:

$$T_c = T_w - \frac{(T_w - T_{sc})\nu_i t}{h_w} \quad (5)$$

where T_{sc} is land surface temperature, ν_i is the velocity of core lifting, and h_w is well depth.

2.1.2. Pressure Field. The state equation, motion equation, continuity equation are shown as follows:²⁷

$$\rho_g = \frac{pM}{RTZ} \quad (6)$$

$$\nu = -\frac{k}{\mu_g} \frac{\partial p}{\partial r} \quad (7)$$

$$\frac{\partial(\rho_g \phi)}{\partial t} + \frac{1}{r} \frac{\partial}{\partial r} (r \rho_g \nu) = 0 \quad (8)$$

where ρ_g is the density of methane, p is pressure, M is the molar mass of methane, R is the universal gas constant, Z is the compressibility factor, ν is the seepage velocity, k is the permeability of core, μ_g is the viscosity of methane, and ϕ is the porosity of core.

Substitute the state equation and the motion equation into the continuity equation.

$$\phi \frac{\partial}{\partial t} \left(\frac{p}{TZ} \right) = \frac{k}{r} \frac{\partial}{\partial r} \left(\frac{pr}{\mu_g TZ} \frac{\partial p}{\partial r} \right) \quad (9)$$

Since p , T are functions of t at the same time Z is the function of p and T , the derivative of a composite function is:

$$\phi \frac{\partial}{\partial t} \left(\frac{p}{TZ} \right) = \phi \left(\frac{p}{TZ} \cdot C_{gT} \frac{\partial p}{\partial t} + \frac{p}{TZ} \cdot C_{gp} \frac{\partial T}{\partial t} \right) \quad (10)$$

where C_{gT} is the isothermal compression coefficient of gas and C_{gp} is the isobaric expansion coefficient of gas.

$$C_{gT} = -\frac{1}{V} \left(\frac{\partial V}{\partial p} \right)_T \quad (11)$$

$$C_{gp} = \frac{1}{V} \left(\frac{\partial V}{\partial T} \right)_p \quad (12)$$

The initial condition is shown as follow:

$$p|_{t=0} = p_w (0 \leq r \leq R_c) \quad (13)$$

where p_w is the well bottom pressure.

The boundary conditions are shown as follows:

$$p_c = p|_{r=r_c} = \rho_f g (h_w - \nu_i t) \quad (t \geq 0) \quad (14)$$

$$p_0 = p|_{r=0} = p_w \quad (t \geq 0) \quad (15)$$

where p_c is core surface pressure, ρ_f is the mud density, p_0 is the core center pressure.

After the calculation of the temperature field and pressure field, the loss of free gas is calculated according to the variation of the core pressure field and temperature field. The cylindrical core is divided into several fan-shaped parts along the axis. Figure 2 shows one of them. Divide the fan-shaped core into n

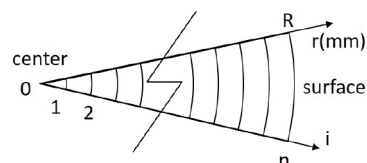


Figure 2. Diagram of the radial division of core.

blocks equidistantly from the center to the surface. Assuming that the area of the first part is 1. The area of block i and its proportion of the fan-shaped core is shown as follows:

$$S_i = 2i - 1 \quad (16)$$

$$P_i = \frac{2i - 1}{1 + 3 + \dots + 2n - 1} \quad (17)$$

where S_i is area of block i , P_i is the block i 's proportion of the fan-shaped core.

According to the theory of molecular thermodynamics, the pore pressure is caused by the thermal movement of free gas.

The relationship between the pressure and the number of molecules is linear. Therefore, in this study, the loss of free gas is calculated based on the pore pressure.

The calculation of the loss of free gas is shown as follow:

$$G_{\text{loss_free}} = \left(\sum_{i=1}^{i=n} \left(\left(\frac{p_0 V_p}{Z_0 R T_0} - \frac{p_i V_p}{Z_i R T_i} \right) \cdot \frac{2i-1}{1+3+\dots+2n-1} \right) \right) \cdot V_m / (V_r \cdot \rho_r) \quad (18)$$

where $G_{\text{loss_free}}$ is loss of free gas during coring, p_0 is initial pressure of core, p_i is the final pressure of block i , T_0 is the initial temperature of the core, T_i is the final temperature of block i , V_p is the volume of pore, V_m is the molar volume of methane at standard conditions, V_r is the volume of core, and ρ_r is the density of core.

Divide both the numerator and denominator by V_r

$$G_{\text{loss_free}} = \left(\sum_{i=1}^{i=n} \left(\left(\frac{p_0 \phi}{Z_0 R T_0} - \frac{p_i \phi}{Z_i R T_i} \right) \cdot \frac{2i-1}{1+3+\dots+2n-1} \right) \right) \cdot V_m / \rho_r \quad (19)$$

The calculation method of the free gas loss has been introduced above. The loss of the adsorbed gas is calculated by isothermal adsorption. According to the theory of isothermal adsorption, the content of adsorbed gas is a monotonically increasing function of pressure, as shown in Figure 3.

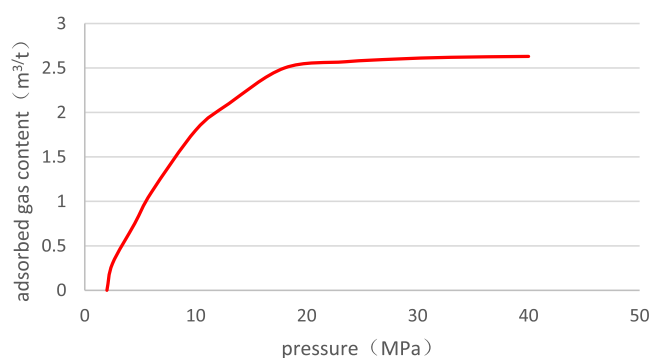


Figure 3. Typical isothermal adsorption curve.

The calculation of the loss of adsorbed gas is shown as follow:

$$G_{\text{loss_ads}} = G_{\text{ads}}(p_2) - G_{\text{ads}}(p_1) \quad (p_2 > p_1) \quad (20)$$

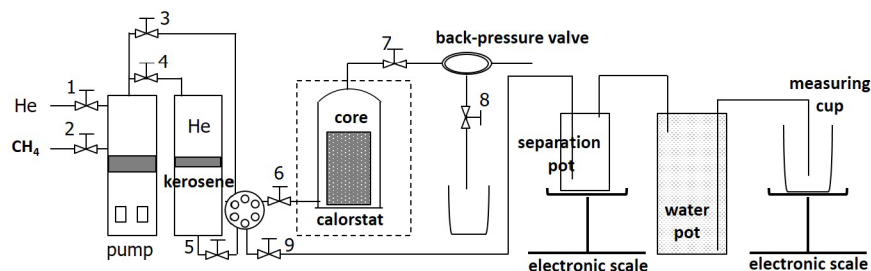


Figure 4. Flow diagram of the in situ gas content test.

where $G_{\text{loss_ads}}$ is the loss of adsorbed gas.

The total loss of gas during coring is shown as follow:

$$G_{\text{loss}} = G_{\text{loss_free}} + G_{\text{loss_ads}} \quad (21)$$

where G_{loss} is the total loss of gas.

The total gas content is:

$$G = G_{\text{loss}} + G_{\text{des}} \quad (22)$$

where G is the total gas content and G_{des} is the on-site desorption gas content.

2.2. Gas Content Prediction Method Based on the In Situ Gas Content Test. In this part, the formation temperature and pressure conditions are created in the laboratory. The core was placed in a sample tank, heated to the original formation temperature, and saturated with methane to the original formation pressure. Wait for several days until the pressure is stable. Add back pressure at the outlet of the sample tank and, at the same time, inject kerosene from the inlet of the sample tank to replace the excess methane and avoid the influence of this part of the methane on the experimental results. A separator tank is arranged between the sample tank and the water tank for separating discharged kerosene and methane. During the experiment, methane in the sample tank is gradually discharged, and the sample tank pressure, water production, and oil production will be recorded too.

According to Yu Lingjie's²⁸ research on shale gas, when the pressure is higher than the saturation pressure the adsorption gas volume does not change much. Based on this phenomenon, Yao Guanghua et al.²⁹ proposed a method for measuring the gas content of shale named the prepressurized test. So in this study, the experiment is repeated twice with different pressures in order to calculate the amount of adsorbed gas and free gas, respectively.

According to the aim of the experiment outlined above, the flow diagram of the in situ gas content test is shown as Figure 4.

The whole steps of the in situ gas content test are as follows:

(1) The core was placed in the sample tank and heated to the original formation temperature. Open valves 2, 3, and 6, pump CH_4 into the tank until the tank pressure reaches the original formation pressure. Wait for several days until the pressure is stable. Close valves 2, 3, and 6.

(2) Add back pressure at the outlet of the sample tank at the same time open the valves 1, 4, 5, 6, 7, and 8, pump kerosene into the tank until no methane is produced at the outlet. Close the valves 1, 4, 5, 6, 7, and 8.

(3) Open the valves 6, 9. Sample tank pressure, gas production, and kerosene production should be recorded during the experiment.

(4) Increase the sample tank pressure and repeat steps (1)2212(3).

Assumed that the free gas content is linearly related to the reservoir pressure. The total gas content can be expressed as follows:²⁹

$$G_1 = A + \frac{p_1 T_s Z_s}{p_s T Z_1} V_p \quad (23)$$

$$G_2 = A + \frac{p_2 T_s Z_s}{p_s T Z_2} V_p \quad (24)$$

where G_1, G_2 is total gas content, p_1, p_2 is the pressure of two experiments, A is adsorption gas content, V_p is volume of pore, T is the temperature of experiments, Z_1, Z_2 is compression factors of two experiments, p_s is the pressure at standard conditions, T_s is the temperature at standard conditions, Z_s is the compression factor at standard conditions.

Let

$$B_1 = \frac{p_1 T_s Z_s}{p_s T Z_1} \quad (25)$$

$$B_2 = \frac{p_2 T_s Z_s}{p_s T Z_2} \quad (26)$$

the total gas content can be expressed as follows:

$$G_1 = A + B_1 V_p \quad (27)$$

$$G_2 = A + B_2 V_p \quad (28)$$

Solve the above equations, A and V_p can be expressed as follows:

$$A = \frac{B_2 G_1 - B_1 G_2}{B_2 - B_1} \quad (29)$$

$$V_p = \frac{G_2 - G_1}{B_2 - B_1} \quad (30)$$

Therefore, the total gas content under any pressure can be calculated using the following formula

$$G = A + B V_p \quad (31)$$

3. RESULTS AND DISCUSSION

In this part, the numerical simulation method and the experiment method mentioned above are used to calculate the in situ gas content of Longmaxi Formation shale in the Sichuan Basin. The basic parameters of the core are shown in Table 1.

Table 1. Basic Parameters of the Shale Core

parameters	value
rate of coring	0.1 m/s
radius	0.05 m
porosity	5%
k	0.0001 mD
depth	3955 m
pressure factor	1.4
reservoir pressure	55 MPa

3.1. Prediction Example of In Situ Gas Content (Numerical Simulation). In this section, two works will be conducted. First, the gas content of the shale mentioned above is calculated by the numerical simulation. And then, the practicability of the mathematical model is analyzed by changing the permeability and coring speed.

3.1.1. Calculation of the Gas Content of Shale. As the shale core approaches the wellhead during the coring process, the variations of core pressure and temperature from the core center to the surface are shown in Figure 5. During coring, the core pressure gradually decreases. And the closer it is to the surface of the core, the more significant the decrease in pressure. The decrease in core temperature also follows the same pattern. Divide the core evenly into 10 parts, from the center to the surface, as shown in Figure 6. Based on the numerical simulations of the temperature field and pressure field, p_0 and p_i are listed in Table 2. Then calculate the gas content according to formula 19. Loss of free gas is 3.78 m³/t, loss of adsorbed gas is 1.04 m³/t, and on-site desorption gas is 0.26 m³/t, so the total gas content is 5.08 m³/t (Figure 7).

3.1.2. Verification of the Mathematical Model. In order to verify the practicability of the numerical model further, in this part, the model is used to analyze the effects of the coring speed and permeability on the loss of gas. The above Longmaxi Formation shale is still taken as an example, as shown in Table 1.

3.1.2.1. Effects of Coring Speed on the Loss of Gas. With other parameters unchanged, the coring speed is set to 0.01, 0.05, 0.1, 1, and 2 m/s in sequence. The variations of core pressure and temperature from the core center to surface are shown in Figures 8 and 9.

The core temperature decreases during coring, and the slower the coring, the more obvious the decrease is. When the coring speed is slower than 0.1 m/s, the heat conduction is sufficient, so the influence of the coring speed on the temperature field is not obvious. With the acceleration of coring speed, the core surface temperature changes rapidly, and the heat conduction is gradually insufficient, so the influence of coring speed on the temperature field becomes obvious. The core pressure decreases during coring, and the slower the coring is, the more obvious the decrease is. Similar to the effect of coring speed on the temperature field, when the coring speed is slower than 0.1 m/s, the effect of coring speed on the pressure field is not obvious, but with the increase of coring speed, the effect gradually appears.

According to the steps described in 3.1.1, as the coring speed gradually increases, the corresponding loss of gas is 4.98m³/t, 4.91m³/t, 4.82m³/t, 3.53m³/t, and 1.88 m³/t, respectively.

3.1.2.2. Effects of Permeability on the Loss of Gas. With other parameters unchanged, the permeability is set to 0.00001, 0.00005, 0.0001, 0.001, and 0.01 mD in sequence. The variations of the core pressure and temperature from the core center to surface are shown in Figures 10 and 11.

The lower the permeability of the core is, the slower the pressure drop is during coring. Cores with permeability of 0.0001, 0.001, and 0.01mD have little difference in the pressure field at the same coring speed, because the mud pressure plays an important role in preventing the gas escape of the core. The change of permeability has no effect on the temperature field.

According to the steps described in 3.1.1, as the permeability gradually increases, the corresponding loss of gas is 3.65m³/t, 4.33m³/t, 4.82m³/t, 4.89m³/t, and 4.97m³/t, respectively.

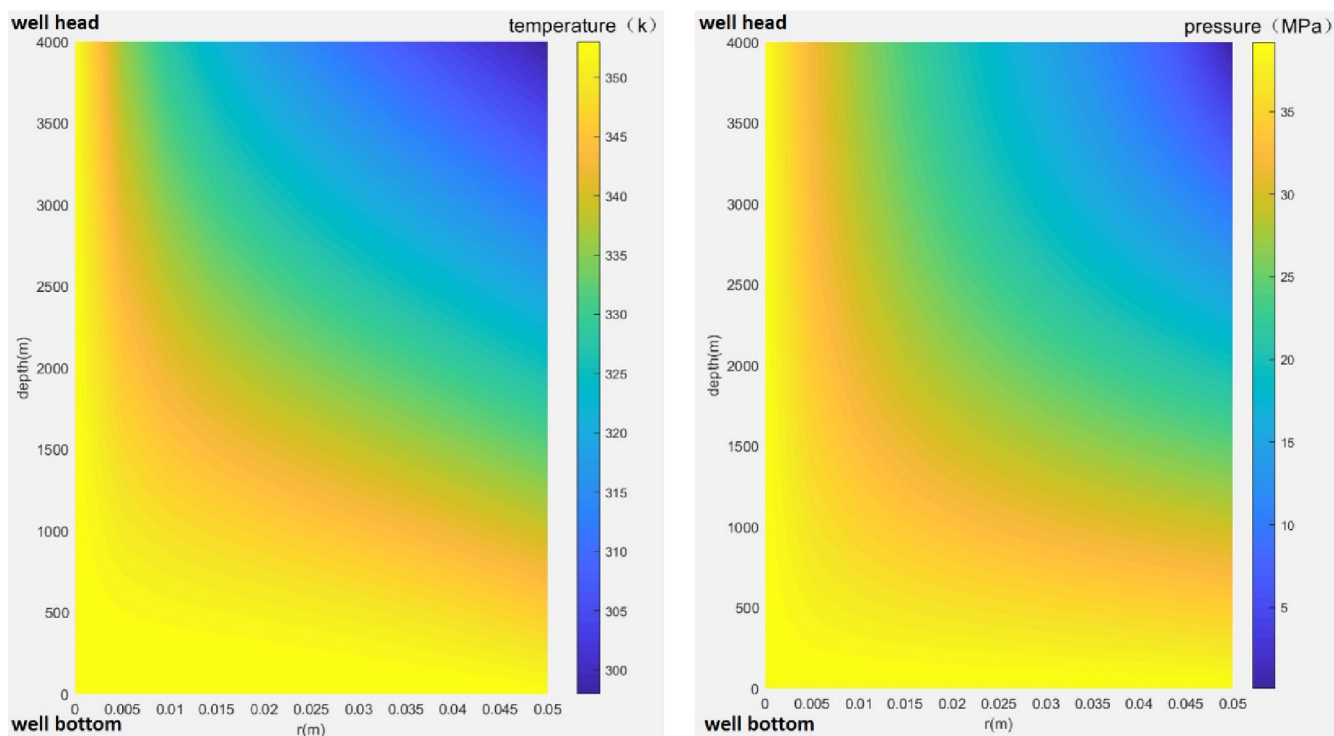


Figure 5. Core pressure and temperature changes during coring.

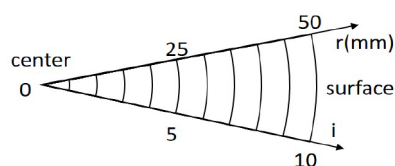


Figure 6. Diagram of radial division of the core in this example.

3.2. Prediction Example of the In Situ Gas Content (Experiment). In this part, the numerical simulation method and the experimental method are used to predict the in situ gas content. The shale of the Longmaxi Formation in the Sichuan Basin is also taken as an example.

Table 3 presents the related data of the two experiments. According to formula 30 and 31, A is $1.226 \text{ m}^3/\text{t}$ and V_p is 0.011 m^3 . Substitute A and V_p with formula 32.

As a result, the total gas content at 55 MPa is $4.95 \text{ m}^3/\text{t}$. Free gas content and adsorbed gas content are $3.72 \text{ m}^3/\text{t}$ and $1.23 \text{ m}^3/\text{t}$, respectively.

3.3. Discussion. First, compare the results predicted by the numerical simulation and experiment with the USBM method and pressure-holding coring. The total gas content predicted

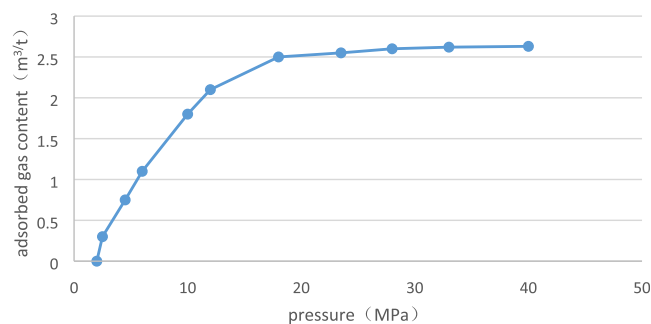


Figure 7. Isothermal adsorption curve of core in this example.

by the numerical simulation of the coring process and the gas content experiment is approximately equal, with values of $5.08 \text{ m}^3/\text{t}$ and $4.95 \text{ m}^3/\text{t}$, respectively, as shown in Figure 12. The total gas content of the USBM method is $4.28 \text{ m}^3/\text{t}$. The total gas content of the pressure-preserved coring is $4.36 \text{ m}^3/\text{t}$.

Due to the limitations of current sealing technology, part of the methane will be lost in the process of pressure-preserved coring. Therefore, the gas content of pressure-preserved coring represents the lower limit of the gas content. The total gas

Table 2. Data Used for Gas Content Calculation Based on the Numerical Simulation of the Coring Process

	i	0	1	2	3	4	5	6	7	8	9	10	total/average
r	mm	0	5	10	15	20	25	30	35	40	45	50	/
percent	/	/	1/100	3/100	5/100	7/100	9/100	11/100	13/100	15/100	17/100	19/100	100/100
p_0	MPa	55	55	55	55	55	55	55	55	55	55	55	/
p_i	MPa	55	44.71	38.05	33.04	28.71	24.73	20.86	16.93	12.69	7.65	0.1	/
$G_{\text{loss_free}}$	m^3/t	0	0.96	1.63	2.19	2.69	3.18	3.66	4.16	4.72	5.40	6.43	3.78
$G_{\text{loss_ads}}$	m^3/t	0	0	0.01	0.02	0.03	0.04	0.08	0.21	0.50	1.18	3.25	1.04
G_{des}	m^3/t	0.26											
G	m^3/t	5.08											

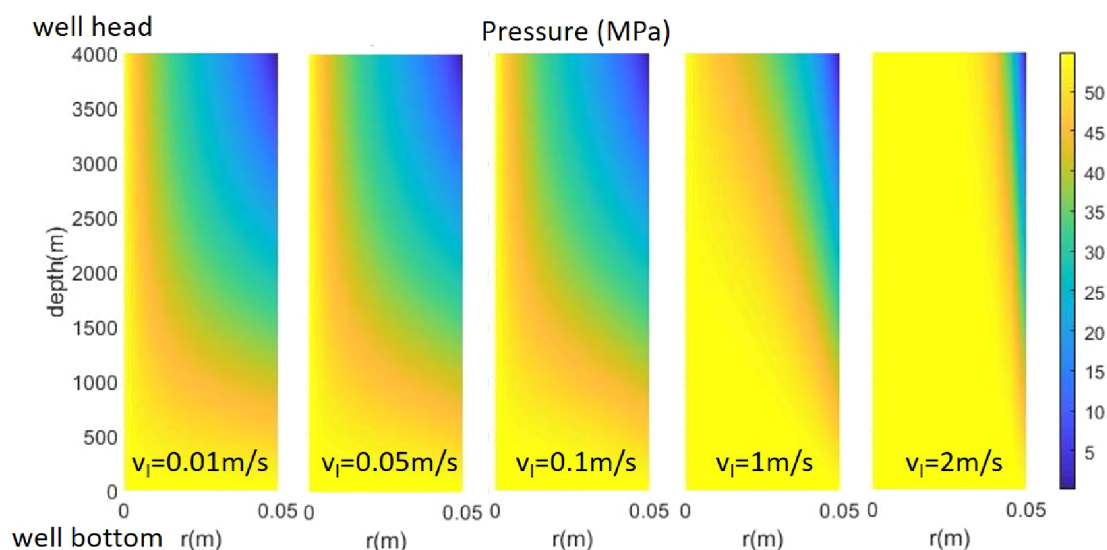


Figure 8. The variations of core pressure at different coring speeds.

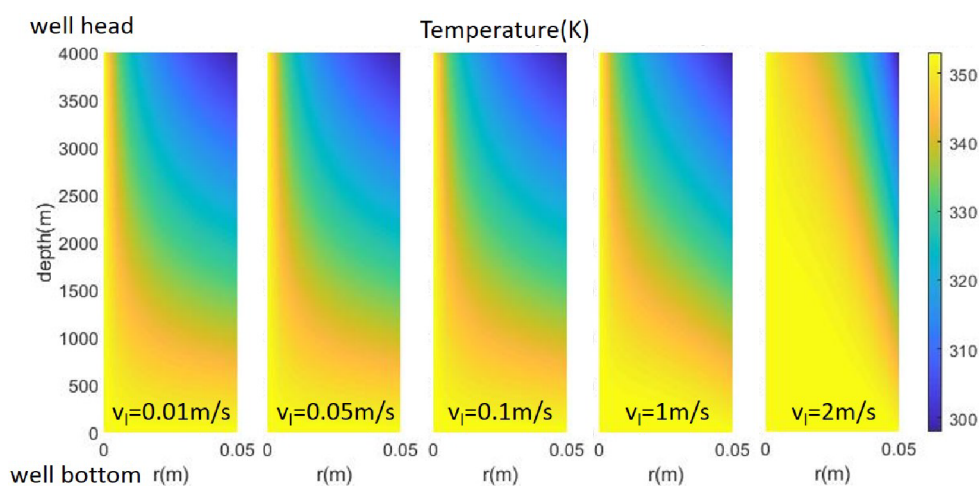


Figure 9. The variations of core temperature at different coring speeds.

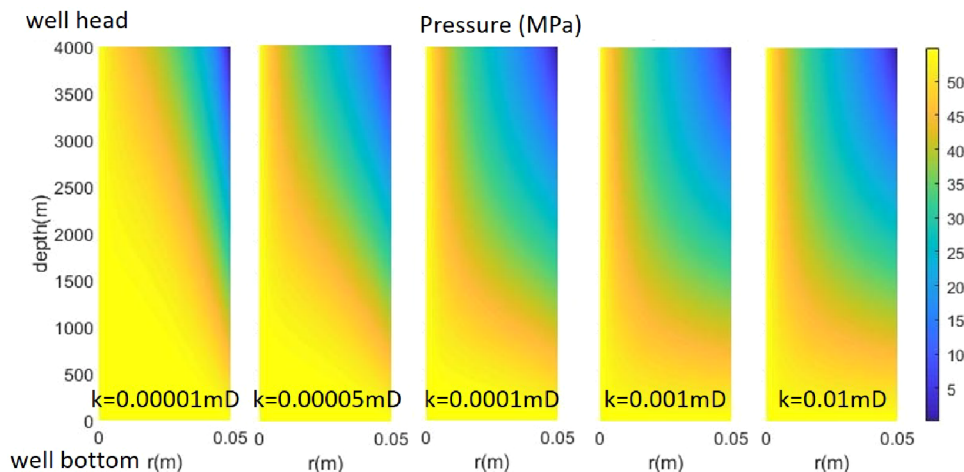


Figure 10. The variations of the core pressure at different permeabilities.

content of the USBM method is lower than that of the pressure-preserved coring method. If using the USBM method for shale with abnormally high pressure, the calculation time of gas loss is later, which might lead to the smaller gas loss.³⁰ The

pressure coefficient is generally high (1.4–2.03) in Longmaxi Formation shale in the Sichuan Basin. So, it can be seen that the USBM method cannot accurately calculate the loss gas for shale. The total gas content predicted by the numerical

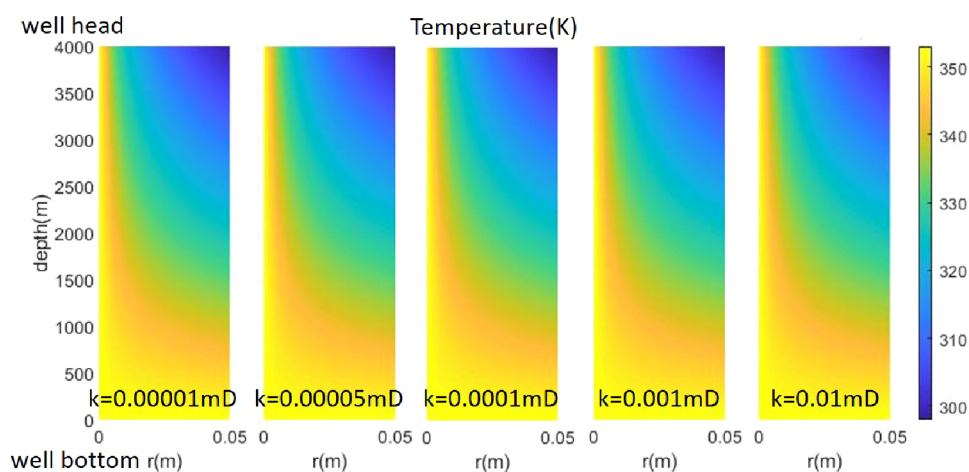


Figure 11. The variations of core temperature at different permeabilities.

Table 3. Data Used for Gas Content Calculation Based on Experiments

	1 _{st}	2 _{nd}
p (MPa)	23	33
T (K)	343	343
G (m ³)	3.312	4.000
Z	0.9245	0.9975
B	198.01	263.31
A (m ³ /t)	1.226	
V_p (m ³)	0.011	

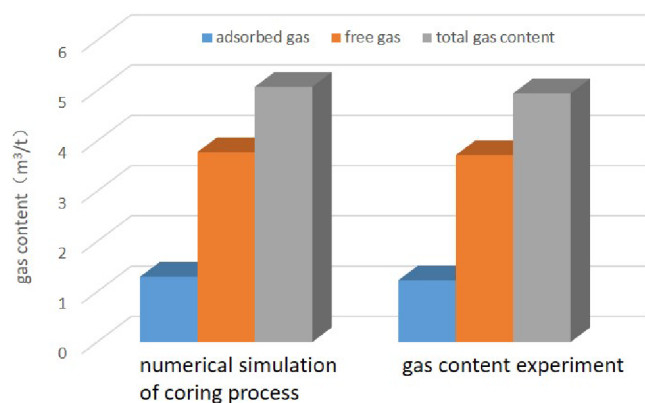


Figure 12. Comparison of results between the two methods.

simulation of the coring process and the gas content experiment is higher than that of the pressure-preserved coring method. This shows that the methods described in this paper can predict the shale gas content reliably.

Second, the numerical model was considered to be reliable by analyzing the effects of coring speed and permeability on the loss of gas. The core temperature decreases during coring, and the slower the coring is, the more obvious the decrease is. The lower the permeability of the core, the slower the pressure drop during coring. These findings indicate that the basic assumptions of the mathematical model in the coring process are valid.

Third, the method of combining experimental and numerical simulation to predict the shale gas content has rarely been reported before. Numerical simulation has a deeper and more detailed understanding of the problem than experiments.

However, the gas content experiment is also a crucial part of the whole method, which confirms the results of the numerical simulation visually.

Nonetheless, there may be a possible limitation in this study. This study does not explore the upper limit of the shale gas content by experiment or numerical simulation. Further research is needed to explore the lower and upper limits of the shale gas content and continue to narrow the gap between them. We believe that this method will continue to improve the accuracy of the shale gas content prediction.

4. CONCLUSIONS

This work aims to provide an in situ gas content prediction method for shale from both mathematical modeling and experiments. First, a gas content prediction method based on the coring process was established using mathematical modeling. Second, another gas content prediction method based on laboratory simulation experiments was established too. Third, in order to verify the practicability of the numerical model, the model is used to analyze the effects of coring speed and permeability on the loss of gas. Finally, the gas content of the Longmaxi Formation shale in the Sichuan Basin is calculated using both methods as an example. The following conclusions can be drawn:

(1) Different from most of the past research, this paper emphasizes the combination of theory and experiment. On the one hand, the theoretical model is verified, and its basic hypothesis is valid. On the other hand, the experiment intuitively reflects the gas content of shale. The mutual verification of theory and experiment makes this method highly reliable.

(2) There is no doubt that the temperature has a significant impact on the calculation of gas content. Compared with previous gas content prediction methods, this article considers the influence of temperature fields on gas content both in mathematical modeling and experiments. The proposed method for gas content prediction contributes to the accurate calculation of the gas content.

(3) The USBM method cannot accurately calculate the loss of gas for shale because of the high pressure coefficient. The gas content of pressure-preserved coring represents the lower limit of the gas content. Further exploration and reduction of the upper and lower limits of shale gas content, to approximate the real gas content, is a direction for future research.

Therefore, the methods described in this paper are highly recommended for the calculations of the gas content. This would be a fruitful area for further work.

AUTHOR INFORMATION

Corresponding Author

Ning Li – Research Institute of Petroleum Exploration and Development, PetroChina, Beijing 100083, China;
 orcid.org/0009-0001-3544-8468; Email: lngpetro@163.com

Authors

Tongwen Jiang – PetroChina Company Limited, Beijing 100007, China

Wei Xiong – Research Institute of Petroleum Exploration and Development, PetroChina, Beijing 100083, China

Complete contact information is available at:
<https://pubs.acs.org/10.1021/acsomega.3c09907>

Notes

The authors declare no competing financial interest.

ACKNOWLEDGMENTS

This research was supported by “Research of shale oil and gas development mechanism and volume development technology” (2023ZZ08), the technology development project of China National Petroleum Corporation.

NOMENCLATURE

T	temperature (K)
t	time from the beginning of coring (s)
r	distance from the core center (m)
T_w	reservoir temperature (K)
r_c	radius of core (m)
T_c	mud temperature (K)
T_{sc}	land surface temperature (K)
v_l	velocity of core lifting (m/s)
h_w	well depth (m)
μ_g	viscosity of methane (mPa·s)
ρ_g	density of methane (kg/m ³)
p	gas pressure in the pore (MPa)
M	molar mass (g/mol)
R	universal gas constant (J/mol·K)
Z	gas compression factor (–)
k	permeability of the core (mD)
ϕ	porosity of the core (–)
v	seepage velocity (m/s)
C_{gT}	isothermal compression coefficient of gas (/MPa)
C_{gp}	isobaric expansion coefficient of gas (/K)
p_w	well bottom pressure (MPa)
p_c	core surface pressure (MPa)
ρ_f	mud density (kg/m ³)
p_0	core center pressure (MPa)
S_i	area of block i (–)
p_i	block i 's proportion of the fan-shaped core (–)
G_{loss_free}	loss of free gas during coring (m ³ /t)
p_0	initial pressure of core (MPa)
p_i	final pressure of block i (MPa)
T_0	initial temperature of core (K)
T_i	final temperature of block i (K)
V_p	volume of pore (m ³)

V_m	molar volume of methane at standard condition (L/mol)
V_r	volume of core (m ³)
ρ_r	density of core (t/m ³)
G_{loss_ads}	loss of adsorbed gas (m ³ /t)
G_{loss}	total loss of gas (m ³ /t)
G	total gas content (m ³ /t)
G_{des}	on-site desorption gas content (m ³ /t)
A	adsorption gas content (m ³ /t)
p_s	pressure at standard condition (MPa)
T_s	temperature at standard condition (K)
Z_s	compression factor at standard condition (–)

REFERENCES

- Yu, L.; Tan, Y.; Fan, M.; Xu, E.; Cui, G.; Pan, Z. Estimating Lost Gas Content for Shales Considering Real Boundary Conditions during the Core Recovery Process. *ACS Omega* **2022**, *7* (24), 21246–21254.
- Zou, C.. *Unconventional Petroleum Geology*; Geological Publishing House, 2011; pp 128164.
- Ma, X.; Wang, H.; Zhou, S.; Shi, Z.; Zhang, L. Deep shale gas in China: Geological characteristics and development strategies. *Energy Rep.* **2021**, *7*, 1903–1914.
- Gou, Q.; Xu, S. Quantitative evaluation of free gas and adsorbed gas content of Wufeng-Longmaxi shales in the Jiaoshiba area, Sichuan Basin, China. *Adv. Geo-Energy Res.* **2019**, *3*, 258–267.
- Bertard, C.; Bruyet, B.; Gunther, J. Determination of desorbable gas concentration of coal (direct method). *Int. J. Rock Mech. Min. Sci. Geomech. Abstr.* **1970**, *7*, 43–65.
- Cao, G.; Zhang, H.; Jiang, W.; Wu, S.; Zhu, D.; Lin, M. A new gas-content-evaluation method for organic-rich shale using the fractionation of carbon isotopes of methane. *SPE J.* **2019**, *24* (6), 2574–2589.
- Schmoker, J. W. Determination of Organic-Matter Content of Appalachian Devonian Shales from Gamma-Ray Logs. *Am. Assoc. Pet. Geol. Bull.* **1981**, *65* (7), 1285–1298.
- Passy, Q. R.; Moretti, F. J.; Kulla, J. B.; Creaney, S.; Stroud, J. D. A practical model for organic richness from porosity and resistivity logs. *Am. Assoc. Pet. Geol. Bull.* **1990**, *74* (12), 1777–1794.
- Jacobi, D. J.; Gladkikh, M.; Lecompte, B.; Hursan, G.; Shoemaker, P.. Integrated Petrophysical Evaluation of Shale Gas Reservoirs. In *SPE Unconventional Resources Conference/Gas Technology Symposium*; SPE, 2008; pp 114925.
- Jacobi, D.; Breig, J.; LeCompte, B.; Kopal, M.; Hursan, G.; Mendez, F.; Bliven, S.; Longo, J.. Effective geochemical and geomechanical characterization of shale gas reservoirs from the wellbore environment: Caney and the Woodford shale. In *SPE Annual Technical Conference and Exhibition*; SPE, 2009; pp 120.
- Zhenhua Tian, S. Z.; Songtao, W.; Sai, X.; Junping, Z.; Jianchao, C. Direct method to estimate the gas loss characteristics and in-situ gas contents of shale. *Gondwana Res.* **2024**, *126*, 40–57.
- Sun, Z.; Shi, J.; Yang, Z.; Wang, C.; Gou, T.; He, M.; Zhao, W.; Yao, T.; Wu, J.; Li, X.. Evaluation about adsorption gas and free gas content inside shale matrix under a wide range of atmosphere conditions. In *Abu Dhabi International Petroleum Exhibition and Conference*; SPE, 2019; pp D031S085R004.
- Hou, X.; Liu, S.; Zhu, Y.; Yang, Y. Evaluation of gas contents for a multi-seam deep coalbed methane reservoir and their geological controls: In situ direct method versus indirect method. *Fuel* **2020**, *265*, 116917.
- Nie, X.; Wan, Y.; Gao, D.; Zhang, C.; Zhang, Z. Evaluation of the in-place adsorbed gas content of organic-rich shales using wireline logging data: A new method and its application. *Front. Earth Sci.* **2021**, *15*, 301–309.
- Bustin, R. M.; Bustin, A. M.; Cui, X.; Ross, D.; Pathi, V. M.. Impact of shale properties on pore structure and storage characteristics. In *SPE Shale Gas Production Conference*; SPE, 2008; pp 119892.

(16) Ross, D. J.; Bustin, R. M. The importance of shale composition and pore structure upon gas storage potential of shale gas reservoirs. *Mar. Pet. Geol.* **2009**, *26* (6), 916–927.

(17) Li, Z.; Ren, T.; Black, D.; Qiao, M.; Abedin, I.; Juric, J.; Wang, M. In-situ gas contents of a multi-section coal seam in Sydney basin for coal and gas outburst management. *Int. J. Coal Sci. Technol.* **2023**, *10* (1), 34–46.

(18) Liu, J.; Bai, X.; Elsworth, D. Evolution of pore systems in low-maturity oil shales during thermal upgrading—Quantified by dynamic SEM and machine learning. *Pet. Sci.* **2023**, 112.

(19) Tang, X.; Jiang, Z.; Jiang, S.; Cheng, L.; Zhang, Y. Characteristics and origin of in-situ gas desorption of the Cambrian Shuijingtuo Formation shale gas reservoir in the Sichuan Basin, China. *Fuel* **2017**, *187*, 285–295.

(20) Junbo, H. *Research on Calculation Method of Shale Gas Loss Basing on the Whole Process of Coring*; Chongqing University, pp 5166

(21) Zhou, S.; Zhang, J.; Zou, C.; Tian, C.; Luo, J.; Zhu, Q.; Jiao, P. A new method for testing shale gas content based on pressure-holding coring technology. *J. China Coal Soc.* **2022**, *47* (4), 1637–1646.

(22) Zou, C.; Dong, D.; Wang, S.; Li, J.; Li, X.; Wang, Y.; Li, D.; Cheng, K. Geological characteristics, formation mechanism and resource potential of shale gas in china. *Pet. Explor. Dev.* **2010**, *37* (6), 641–653.

(23) Zhou, C.; Dong, D.; Yang, H.; Wang, Y.; Huang, J.; Wang, S.; Fu, C. Conditions of Shale Gas Accumulation and exploration practices in China. *Nat. Gas Ind.* **2011**, *31* (12), 26–39.

(24) Wu, K.; Chen, Z.; Li, X.; Guo, C.; Wei, M. A model for multiple transport mechanisms through nanopores of shale gas reservoirs with real gas effect—adsorption-mechanic coupling. *Int. J. Heat Mass Transfer* **2016**, *93* (2), 408–426.

(25) Bin, Z. *Study on Seepage Law of Shale Gas Reservoir Considering Desorption and Deformation of Organic Matter*; Xi'an Shiyou University, 2023; 815.

(26) Gu Chaohao, L. D.; Nuxing, C.; Songmu, Z.; Yongji, T. *Equations of Mathematical Physics*; Higher Education Press, 2012; pp 4770.

(27) Jiali, G. *The Modern Mechanics of Fluids Flow in Reservoir*; Petroleum Industry Press, 2003; *1*, 50–80

(28) Yu Lingjie, F. M.; Hongyu, C.; Weixing, L.; Wentao, Z.; Ershe, X. Isothermal adsorption experiment of organic-rich shale under high temperature and pressure using gravimetric method. *Acta Phys. Sin.* **2015**, *36* (5), 557–563.

(29) Guanghua, Y.; Wei, X.; Yun, X.; Xiaoquan, W.; Wei, Y.; Weijun, D.; Hongyu, D.; Qisen, G. A new method of pre-pressurized test on shale gas content. *Acta Pet. Sin.* **2017**, *38* (10), 1189–1193.

(30) Guanghua, Y.; Xiaoquan, W.; Hongyu, D.; Wei, Y.; Mei, G.; Rui, X.; Zhiqiang, L. Applicability of USBM method in the test on shale gas content. *Acta Pet. Sin.* **2016**, *37* (6), 802–806.